Zinc-substituted myoglobin is a naturally occurring photoantimicrobial agent with potential applications in food decontamination

Zinc-substituted myoglobin is a naturally occurring photoantimicrobial agent with potential applications in food decontamination

Pietro Delcanale,[a] *Chiara Montali,* [a] *Beatriz Rodríguez-Amigo,* [b] *Stefania Abbruzzetti,* [c,d] *Stefano Bruno,* [e] *Paolo Bianchini,*[f] *Alberto Diaspro,* [f] *Montserrat Agut,* [b] *Santi Nonell,* [b,*] *Cristiano Viappiani* [a,d,*]

[a] Dipartimento di Fisica e Scienze della Terra, viale delle Scienze 7A, 43124, Parma, Italy.

[b] Institut Quimic de Sarrià, Universitat Ramon Llull, Via Augusta 390, 08017 Barcelona, Spain

[c] Dipartimento di Bioscienze, viale delle Scienze 11A, 43124, Parma, Italy.

[d] NEST, Istituto Nanoscienze, Consiglio Nazionale delle Ricerche, Piazza San Silvestro 12, 56127 Pisa, Italy.

[e] Dipartimento di Farmacia, viale delle Scienze 23A, 43124, Parma, Italy.

[f] Fondazione Istituto Italiano di Tecnologia, Via Morego, 30, 16163 Genova, Italy.

Corresponding authors: Cristiano Viappiani Tel. +39 0521 905208, Fax+39 0521 905223, Email cristiano.viappiani@unipr.it; Santi Nonell Tel. +34 932 672 000, Fax: +34 932 056 266, Email: santi.nonell@iqs.url.edu.

17 Keywords: Antibacterial photosensitization-based treatment, natural photosensitizers, singlet
18 oxygen

19 ABSTRACT Zinc-substituted myoglobin (ZnMb) is a naturally-occurring photosensitizer that
20 generates singlet oxygen with a high quantum yield. Using a combination of photophysical and
21 fluorescence imaging techniques, we demonstrate the interaction of ZnMb with Gram positive
22 *Staphylococcus aureus* and Gram negative *Escherichia coli.* An efficient antibacterial action
23 against *S. aureus* was observed, with a reduction up to 99.9999% in the number of colony
24 forming units, while no sizeable effect was detected against *E. coli*. Since ZnMb is known to
25 form during the maturation of additive-free not-cooked cured ham, the use of this protein as
26 built-in photodynamic agent may constitute a viable method for the decontamination of these
27 food products from Gram-positive bacteria.

28

Introduction

Effective decontamination of food and food processing tools and environments is one of the major open issues in current food science. Novel methods are currently being searched with minimal effects on food quality while still warranting the complete removal of dangerous pathogens. In this context, antibacterial photosensitization-based treatments are gaining attention thanks to their unique properties. [1,2] Photosensitization is a light-activated reaction where a photo-excited chromophore, called a photosensitizer (PS), reacts with molecular oxygen (O_2) to produce reactive oxygen species (ROS). The cytotoxicity of the ROS produced by photosensitization can be usefully exploited to inactivate microbial cells. [3,4] Among ROS, the non-radical and non-ionic electronically-excited state of the dioxygen molecule, called singlet oxygen ($^1O_2$), plays a crucial role in the photo-induced damage of the cells. $^1O_2$ is indeed highly reactive and rapidly oxidizes substrates like membrane lipids, proteins or nucleic acids, when produced in or near a cell. [5] An additional strength of the photodynamic approach relies on the observation that no resurgence of photo-resistant species occurs even after multiple exposures. [3,6]

The efficacy of a PS is highly dependent on its bioavailability and biocompatibility, as well as on its affinity for the target cells. Novel materials and biomaterials have recently become available with properties that comply with these requirements and, in addition, enable their detection and monitoring. [7]

Despite PSs can be found in several classes of molecules, [8] only a few examples of protein-based PS have been reported. Variants of the Green Fluorescent Protein (GFP) family, [9,10] the protein “killer RED” [11] [12] and the flavoprotein “mini Singlet Oxygen Generator” (miniSOG) [13,14] are relevant examples of genetically-encoded PS, but characterized by a low quantum yield of $^1O_2$ production (Φ_Δ=0.004±0.001 for Enhanced-GFP and 0.03±0.01 for miniSOG). An

alternative approach is the use of protein-based carriers as they may confer water-solubility and bio-compatibility to hydrophobic PSs, along with the benefits of a nano-metric size. Widespread proteins like apo-myoglobin (apoMb), i.e. the protein portion of myoglobin (Mb), or β-lactoglobulin (βLG) have been recently proposed as carriers for the natural hydrophobic PS hypericin (Hyp). [15,16] The binding of Hyp to the hydrophobic pocket of these proteins leads to a remarkable increase of its quantum yields of $^1O_2$ photosensitization ($\Phi_\Delta \approx 0.1$) and fluorescence emission (Φ_F) in biological media. The latter property was recently exploited to collect STimulated Emission Depletion (STED) images of PS loaded bacteria, thus allowing a precise sub-diffraction localization of the PS in living cells. [17] However, the relatively weak interaction occurring between Hyp and such protein hosts limits the usefulness of these particular complexes since Hyp can translocate to e.g., serum proteins in real biological systems. In contrast, Lepeshkevich et al. recently studied the photosensitized production of $^1O_2$ from ZnMb, where a high value for the Φ_Δ (0.9±0.1) was obtained by substituting the iron ion in the center of the heme cofactor of Mb with a Zn(II) ion. [18] In this case, the zinc-protoporphyrin IX cofactor is also bound to the protein matrix by means of a coordinate bond. It is particularly interesting that zinc-protoporphyrin IX spontaneously forms as ZnMb [19,20] during the maturation of nitrate/nitrite-free dry cured ham. [21-24] Since these products are not-cooked and are additive-free, they easily suffer from bacterial contaminations. In view of the above, we hypothesized that the built-in PS ZnMb could potentially be exploited as antimicrobial agent for such hams, avoiding the introduction of exogenous products for disinfection purposes or preservative agents. In this work, we focused on the study of the interaction of ZnMb with two representative bacteria, Gram-positive *Staphylococcus aureus* and Gram-negative *Escherichia coli*, and evaluated its photoinactivation ability.

Materials and Methods

Zinc-protoporphyrin IX (ZnPP IX) and Mb from horse heart were purchased from Sigma-Aldrich and used as received.

apoMb preparation and reconstitution with ZnPP IX

The apo-form of Mb was prepared removing heme from myoglobin by the methyl ethyl ketone method. [25] The concentration of the apoMb stock was calculated from the absorption at 280 nm (ε=15 800 cm^{-1} M^{-1}), while residual heme concentration was estimated from the absorption at 408 nm (ε = 179 000 cm^{-1} M^{-1}). [26] In all preparations, heme contamination was typically 1% of the total protein content.

To reconstitute ZnPP IX into apoMb, ZnPP IX was dissolved in a 10 mM NaOH solution and added dropwise to a Phosphate Buffer Saline (PBS) solution of apoMb until an equimolar concentration was reached. The whole procedure was carried out at 4 °C under dim light and the solution was kept in the dark with continuous and gentle stirring for 24 h. The sample was then centrifuged and the supernatant was dialyzed against a PBS buffer solution. The obtained ZnMb stock solution was spectroscopically checked to assess sample purity. A 1:1 stoichiometry between ZnPP IX and apoMb was regularly observed. The concentration was calculated from the absorption at 554 nm (ε=10 400 cm^{-1} M^{-1}). [18]

General spectroscopic instrumentation

Absorption spectra recorded using a Jasco V-650 (Jasco Europe, Carpi, Italy). Fluorescence spectra were recorded using a Spex-Fluoromax 4 (Horiba Jobin Yvon, Edison, NJ) or a Perkin Elmer LS50 spectrofluorometers (PerkinElmer, Waltham, MA).

Fluorescence and transmitted light microscopy

Cell suspensions in sterile PBS were drop-casted on a coverslip and imaged by means of an A1r MP NIKON confocal microscope (Nikon Instruments, Tokyo, Japan). The samples were excited at 561 nm focusing a laser beam through a Plan Apo vc 100× 1.4NA oil immersion objective. The fluorescence was collected by the same lens and detected in the spectral window between 600 and 670 nm by means of a GaAsP photomultiplier tube (PMT), while the transmitted laser light was detected by a PMT through a condenser lens.

Fluorescence correlation spectroscopy and time-resolved fluorescence

Fluorescence Correlation Spectroscopy (FCS) and time-resolved fluorescence (TRF) experiments were performed using a Microtime 200 system from PicoQuant, based on an inverted confocal microscope (Olympus IX70) and equipped with two single photon avalanche diodes (SPADs). Excitation was achieved by a 475 nm picosecond diode laser. Fluorescence emission by ZnMb was collected through a bandpass filter (650 nm-700 nm) and split with a 50/50 splitter between the two detection channels. A time-correlated single photon counting (TCSPC) operation mode was used for TRF measurements; and a cross-correlation mode was used for FCS measurements. In order to study the interaction of ZnMb with bacteria, either *E. coli* or *S. aureus* suspensions were added to the protein solution. Bacteria suspensions with an optical density at 600 nm corresponding to 0.4 were further diluted 100-fold. Solutions were incubated for 10 minutes before performing the experiment.

Laser flash photolysis (LFP)

Triplet state decays of ZnMb were monitored at 465 nm after photoexcitation with the second harmonic (532 nm) of a nanosecond Nd:YAG laser (Spectron Laser) using a previously described setup. [27] The effect on triplet state due to the interaction between ZnMb and bacteria was assessed by diluting ZnMb (final concentration 2 or 5 μM) in bacteria suspensions (*E. coli*

or *S. aureus*) with an optical density of 0.4 at 600 nm. Solutions were incubated for 10 minutes before performing the experiment.

Singlet oxygen measurements

Time-resolved near-infrared spectroscopy (TRNIR) was used to monitor $^1O_2$ phosphorescence at 1275 nm using a modified PicoQuant Fluotime 200 system. The setup uses a diode-pumped pulsed Nd:YAG laser for excitation (FTSS355-Q, Crystal Laser, Berlin, Germany; 1kHz repetition rate, λ_{exc} = 532 nm, 1.2 μJ per pulse) and a photon counting module (H9170-45 NIR-PMT, Hamamatsu) coupled to a multichannel scaler (NanoHarp 250, PicoQuant, Germany) for detection. The time-resolved phosphorescence signals were fitted with equation (1):

$$S = S_0 \frac{\tau_\Delta}{\tau_\Delta - \tau_T}\left(e^{-t/\tau_\Delta} - e^{-t/\tau_T}\right) + y_0 \qquad (1)$$

where τ_T and τ_Δ are the lifetime of the photosensitizer triplet state and of $^1O_2$ respectively, y_0 is an offset due to instrument dark counts and s_0 is an instrumental quantity proportional to Φ_Δ [28].

Microbial strains and growth conditions

S. aureus CECT 239 and *E. coli* CECT 101, obtained from the Spanish Type Culture Collection (CECT), were grown overnight in sterile Tryptic Soy Broth (TSB) or in Luria Bertani medium (LB) at 37°C. Stock inoculum suspensions were prepared in sterile PBS and adjusted to an optical density of 0.4 at 600 nm.

Photodynamic inactivation of S. aureus and E. coli

Cell suspensions in sterile PBS were incubated for 30 min in the dark at room temperature with the PS. The final concentration of the PS in the cell suspensions ranged between 0 and 50 μM. Then, 0.3 mL of the suspensions were placed in 96-well plates. The plates were illuminated from the top with green light (LED, 520 nm) for 15 or 30 min (18 and 37 J cm^{-2}, respectively, measured with a calibrated power meter), serially diluted, seeded on tryptic soy agar, and

incubated in the dark for 24 h at 37 °C. Colony-forming units (CFUs) were counted in order to calculate the survival fraction. Experiments were carried out in duplicate for each condition, including cell controls without the addition of PS and dark controls.

Results and discussion

Photophysical properties of ZnMb in PBS solution

The absorption and fluorescence emission spectra of ZnMb in PBS buffer at 20 °C closely match those reported in the literature. [18] The absorption spectrum of the protein is characterized by an intense Soret band centered at 428 nm and two Q-bands, about 16-times weaker, centered at 554 and 595 nm (Figure 1). The fluorescence emission spectrum shows an intense narrow band with a maximum at 597 nm and a broader, less intense emission band around 650 nm (Figure 1).

Fluorescence decay occurs with a single exponential decay with lifetime τ_F = 2.0±0.1 ns (Table 1). The triplet-state lifetime (τ_T), measured by monitoring the transient triplet-triplet absorption at ~465 nm, ranges from 26±1 μs in air-equilibrated PBS to 13±1 ms in deaerated solutions (Table 1), in agreement with previous determinations. [18,29] Compared to τ_T of typical PSs in air-saturated aqueous solutions (2-3 μs), [30] τ_T is substantially longer, which indicates that ZnMb is somewhat more shielded from oxygen, in agreement with the localization of the porphyrin within the protein cavity. τ_T values determined by TRNIR (eq. 1) were in good agreement, with small differences being due to minor differences in experimental conditions. In turn, the singlet oxygen decay lifetimes were also consistent with literature values for similar systems. [15,16] All the above photophysical parameters are likewise consistent with the values previously reported for ZnMb in 50 mM citrate-phosphate buffer pH=7.4. [18]

Interaction between ZnMb and bacterial cells

The remarkable $^1O_2$ photosensitizing efficiency of ZnMb suggests that this compound could be exploited to obtain efficient bacterial photoinactivation.

Direct demonstration of the interaction between ZnMb and bacterial cells was obtained by exploiting the fluorescence emission of the compound to collect images through a confocal microscope. *S. aureus* and *E. coli* suspensions were incubated with 1 μM ZnMb for 10 minutes prior to image collection. Comparison of the confocal images with those obtained in transmitted light mode clearly shows accumulation of the fluorescent ZnMb both on *S. aureus* (Figure 2, panels A-C) and *E. coli* (Figure 3, panels A-C). Washed samples show a substantial reduction of the protein's fluorescence from both *S. aureus* (Figure 2, panels D-F) and *E. coli* (Figure 3, panels D-F), which becomes barely distinguishable from the background. This fact indicates that the interaction between the protein and the bacterial cell wall is rather weak, ZnMb internalization being negligible.

Incidentally, we noticed that attempts to exploit the inherent fluorescence emission by ZnMb to reach subdiffraction resolution using a STED microscope failed, possibly because of the low fluorescence yield and transient absorption properties of the compound.

Further evidence for the existence of spontaneous interactions between ZnMb and bacterial cells was provided by FCS measurements. The fluorescence intensity time-traces from *E. coli* and *S. aureus* suspensions incubated with ZnMb (~1 μM) were characterized by several spikes, corresponding to very slow diffusing species at low (~nM) concentration, that are reasonably identified with bacteria, decorated with several copies of ZnMb. An analysis of the cross-correlation curves calculated on the spikes led to an estimate of the diffusion coefficient D for

these species: (0.10±0.05) $\mu m^2/s$ and (0.3±0.1) $\mu m^2/s$ for ZnMb incubated with *E. coli* and *S. aureus*, respectively (Table 1). According to the Stokes-Einstein equation for spherical particles, these values correspond to diffusing species of radius ~2 and ~0.7 μm, respectively, roughly in keeping with the expected size of the investigated bacterial cells. The radius for *E. coli* must be considered as a rough estimate, since the bacteria are rod shaped and not spherical.

No substantial changes in the photophysical properties of ZnMb could be observed when the compound was bound to the cells (Table 1), except for a slight increase of the triplet lifetime τ_T in the presence of *S. aureus* (from 26±1 μs to 34±3 μs). The larger value of τ_T may result from a reduced accessibility of O_2 to the protein pocket, possibly caused by an interaction with the cell wall. The value of τ_T for ZnMb incubated with *E. coli* is 29±3 μs, larger but still consistent with the one obtained in the absence of bacteria. The assignment of the transient absorption to the triplet state was confirmed by the increase of its lifetime upon removal of oxygen from samples (Table 1).). It should be noted that a related porphyrin photosensitiser, Photofrin, showed a shorter triplet lifetime (6 μs) when bound to S. aureus , which suggests that the ZnPPIX chromophore remains bound to myoglobin. [31]

Figure 4 compares the fluorescence emission spectra and the $^1O_2$ phosphorescence kinetics obtained for ZnMb in solution and incubated with bacterial cells. The results are similar for both *S. aureus* (panels A - B) and *E. coli* (panels C – D): after the incubation with the cells (blue curves), both fluorescence emission and $^1O_2$ phosphorescence kinetics are substantially unchanged with respect to ZnMb in PBS (black curves). Thus, the protein's ability to photosensitize the production of $^1O_2$ appears to be unaltered by the presence of the cells.

Additional experiments were carried out washing the sample after the incubation period, by means of centrifugation and re-suspension of the pellet in fresh PBS buffer. No sizeable ZnMb

fluorescence nor $^1O_2$ phosphorescence emission was detected for the washed samples (red curves), confirming the conclusions of the imaging data, namely that the interaction between ZnMb and the bacteria is relatively weak.

Accordingly, fluorescence emission from the supernatant (green curves) is almost indistinguishable from that observed before centrifugation, an indication that ZnMb dissociated from the bacterial wall upon centrifugation.

Photodynamic inactivation

Photodynamic inactivation of bacteria by green-light irradiation of ZnMb was tested at different protein concentrations and at different light fluences for *S. aureus* (Figure 5 panel A and B) and *E. coli* (Figure 5 panels C and D). A substantial difference in the efficacy of the photo-inactivation on the two strains can be immediately recognized: while *S. aureus* were efficiently inactivated, with a reduction in the number of bacterial colony forming units (CFU) up to 6 logarithmic units, *E. coli* was not affected by the photodynamic treatment. The reason for this opposite response of the two strains is very likely related to the different structure of the corresponding bacterial cell walls.

The Gram-negative *E. coli* are characterized by a more complex cell wall in comparison to the Gram-positive *S. aureus*, with an outer impermeable membrane that counteracts the action of the photosensitizer, by preventing the diffusion to the sensitive inner membrane [32]. Given the short diffusion of $^1O_2$ in the cellular environment, limited to at most ~200 nm from the site of photosensitization, [33] $^1O_2$ that is produced on the surface of *E. coli* cells is unable to induce a

lethal damage, probably because the outer membrane is more protective against the produced $^1O_2$.

Despite the observed accumulation of ZnMb on both cells types, the PS is able to photoinativate only the Gram positive *S. aureus*, as reported for other protein based PSs, like the complexes between Hyp and apoMb, [16] [17] or β-lactoglobulin. [15] Unlike the developed protein based PSs, there are several examples that proved effective against Gram negative bacteria, including, e.g. cationic PSs like methylene blue and toluidine blue, derivatives of phthalocyanines, chlorins, porphyrins, chlorophyll, functionalized fullerenes and nanoparticles. [32]

As discussed above, this result is consistent with the presence of a weak interaction between ZnMb and the cells leading to a localization of the protein only at the cells surface. Since the isoelectric point of myoglobin is 7.2, the net charge on the protein is essentially zero (-0.5). Thus, ionic interactions between the protein and the bacteria wall surface are not expected to influence substantially the binding process.

S. aureus disinfection (3-logs CFU reduction, 99.9%) could be achieved with a ZnMb concentration of 3 μM and a light fluence of 18 J/cm^2. The most efficient conditions for *S. aureus* photo-inactivation were obtained by increasing the protein concentration to 20 μM and the light fluence to 37 J/cm^2, which allowed to decrease the *S. aureus* population by 99.9999% (6 logs), without appreciable dark toxicity. The administration of an even higher concentration of ZnMb (50 μM) induced some dark toxicity and resulted less efficient in the photo-inactivation than the lower concentrations, particularly for the lower light dose. This effect was attributed to a screening (inner filter) effect due to the major absorption of light by the protein in solution, as already observed for other systems with high PS concentration. [34]

Importantly, already at the lowest ZnMb concentration employed (3 μM) the reduction in CFU amounts to 4-log units at 18 J/cm^2, and reaches 5-log units at 37 J/cm^2. This concentration is comparable to the one estimated in ham, ranging between 1.6 and 2.8 μM. [22]

The above results can be compared with those we have obtained with other protein-based photosensitizers. The same protein scaffold (apomyoglobin, i.e. the protein portion of myoglobin where the heme was removed) was used to host the naturally occurring photosensitizer hypericin in the heme cavity. [16] This complex proved effective against *S. aureus* and was able to induce a 5-log reduction. Similarly, the complex between hypericin and β-lactoglobulin was found to be effective on *S. aureus*, leading to a 5-log decrease upon exposure to a light dose of 20 J. [15]

The photodynamic action of ZnMb on *S. aureus* can be compared to the effect reported for the cofactor ZnPP IX in the absence of a carrier by Ishikawa *et al*. [35] Under experimental conditions that are similar to ours, the survival of *S. aureus* appears to be a bit higher, possibly because of the tendency of ZnPP IX towards aggregation and the presence of two negative charges on its structure, that preclude cell-wall binding due to electrostatic repulsion. Thus, we conclude that the use of the protein carrier leads to an improvement in the efficiency of ZnPP IX alone.

The above results demonstrate that ZnMb is a promising natural photosensitizing agent that is found in cured ham. It is endowed with a very large capacity to photosensitize the production of $^1O_2$ upon exposure to harmless visible light. It spontaneously accumulates on bacterial cells of *S. aureus* and *E. coli* species and is an effective PDT agent capable of reducing the population of Gram-positive *S. aureus* up to 6 log CFU with no appreciable dark toxicity. Conversely, the Gram-negative *E. coli* was unaffected by the PDT treatment with ZnMb in all the conditions tested. This study demonstrates the possibility to employ ZnMb as a bio-compatible PS for the inactivation of Gram-positive bacteria. This nano-metric size, bio-compatible protein structure is

particularly interesting for its potential application in the decontamination of non-cooked, additive-free cured ham because it is spontaneously produced during the maturation. Experiments with contaminated food (hams) and food handling materials will assess the feasibility of the approach in industrial applications.

Corresponding Author

* Cristiano Viappiani Dipartimento di Fisica e Scienze della Terra, viale delle Scienze 7A, 43124, Parma, Italy. Email: cristiano.viappiani@unipr.it; Santi Nonell, Institut Quimic de Sarrià, Universitat Ramon Llull, Via Augusta 390, 08017 Barcelona, Spain. Email: santi.nonell@iqs.url.edu

Author Contributions

The manuscript was written through contributions of all authors. All authors have given approval to the final version of the manuscript.

Funding Sources

This work has been supported by the Spanish Ministry of Economy and Competitiveness by Grant No. CTQ2013-48767-C3-1-R. CV acknowledges funding by University of Parma. The authors acknowledge financial support from Nikon Imaging Center at the Fondazione Istituto Italiano di Tecnologia.

ACKNOWLEDGMENT

CV acknowledges Silvia Braslavsky for the kind donation of the Spectron laser used in flash photolysis experiments.

302 REFERENCES

303 (1) Luksiene, Z.; Brovko, L. Antibacterial Photosensitization-Based Treatment for
304 Food Safety *Food Engineering Reviews* **2013**, *5*, 185-199.
305 (2) Tortik, N.; Steinbacher, P.; Maisch, T.; Spaeth, A.; Plaetzer, K. A comparative
306 study on the antibacterial photodynamic efficiency of a curcumin derivative and a formulation on
307 a porcine skin model *Photochemical & Photobiological Sciences* **2016**, *15*, 187-195.
308 (3) Dai, T.; Huang, Y.-Y.; Hamblin, M. R. Photodynamic therapy for localized
309 infections - State of the art *Photodiagnosis and Photodynamic Therapy* **2009**, *6*, 170-188.
310 (4) Jori, G.; Camerin, M.; Soncin, M.; Guidolin, L.; Coppellotti, O. In *Photodynamic*
311 *Inactivation of Microbial Pathogens: Medical and Environmental Applications*; Hamblin, M. R.,
312 Jori, G., Eds.; The Royal Society of Chemistry: 2011; Vol. 11, p 1-18.
313 (5) Cló, E.; Snyder, J. W.; Ogilby, P. R.; Gothelf, K. V. Control and Selectivity of
314 Photosensitized Singlet Oxygen Production: Challenges in Complex Biological Systems
315 *ChemBioChem* **2007**, *8*, 475-481.
316 (6) Kharkwal, G. B.; Sharma, S. K.; Huang, Y. Y.; Dai, T.; Hamblin, M. R.
317 Photodynamic therapy for infections: clinical applications *Lasers Surg Med.* **2011**, *43*, 755–767.
318 (7) Planas, O.; Boix-Garriga, E.; Rodríguez-Amigo, T., J.B.; Bresolí-Obach, R.;
319 Flors, C.; Viappiani, C.; Agut, M.; Ruiz-González, R.; Nonell, S. In *Photochemistry*; Albini, A.,
320 Fasani, E., Eds.; The Royal Society of Chemistry: London, 2014; Vol. 42.
321 (8) DeRosa, M. C.; Crutchley, R. J. Photosensitized singlet oxygen and its
322 applications *Coordination Chemistry Reviews* **2002**, *233â€“234*, 351-371.
323 (9) Jimenez-Banzo, A.; Nonell, S.; Hofkens, J.; Flors, C. Singlet Oxygen
324 Photosensitization by EGFP and its Chromophore HBDI *Biophysical Journal* **2008**, *94*, 168–172.

(10) Jiménez-Banzo, A.; Ragàs, X.; Abbruzzetti, S.; Viappiani, C.; Campanini, B.; Flors, C.; Nonell, S. Singlet oxygen photosensitisation by GFP mutants: Oxygen accessibility to the chromophore *Photochemical and Photobiological Sciences* **2010**, *9*, 1336-1341.

(11) Bulina, M. E.; Chudakov, D. M.; Britanova, O. M.; Yanushevic, Y. G.; Staroverov, D. B.; Chepurnikh, T. V.; Merzlyak, E. M.; Shkrob, M. A.; Lukyanov, S.; Lukyanov, K. A. A genetically encoded photosensitizer *Nature Biotechnology* **2006**, *24*, 95-99.

(12) Vegh, R. B.; Solntsev, K. M.; Kuimova, M. K.; Cho, S.; Liang, Y.; Loo, B. L. W.; Tolbert, L. M.; Bommarius, A. S. Reactive oxygen species in photochemistry of the red fluorescent protein "Killer Red" *Chemical Communications* **2011**, *47*, 4887-4889.

(13) Ruiz-Gonzalez, R.; Cortajarena, A. L.; Mejias, S. H.; Agut, M.; Nonell, S.; Flors, C. Singlet Oxygen Generation by the Genetically Encoded Tag miniSOG *Journal of the American Chemical Society* **2013**, *135*, 9564-9567.

(14) Pimenta, F. M.; Jensen, R. L.; Breitenbach, T.; Etzerodt, M.; Ogilby, P. R. Oxygen-Dependent Photochemistry and Photophysics of “MiniSOG,” a Protein-Encased Flavin *Photochemistry and Photobiology* **2013**, *89*, 1116-1126.

(15) Rodríguez-Amigo, B.; Delcanale, P.; Rotger, G.; Juárez-Jiménez, J.; Abbruzzetti, S.; Summer, A.; Agut, M.; Luque, F. J.; Nonell, S.; Viappiani, C. The complex of hypericin with β-lactoglobulin has antimicrobial activity with perspective applications in dairy industry *Journal of Dairy Science* **2015**, *98*, 89–94.

(16) Comas-Barceló, J.; Rodríguez-Amigo, B.; Abbruzzetti, S.; Rey-Puech, P. d.; Agut, M.; Nonell, S.; Viappiani, C. A self-assembled nanostructured material with photosensitising properties *RSC Advances* **2013**, *3*, 17874-17879.

(17) Delcanale, P.; Pennacchietti, F.; Maestrini, G.; Rodríguez-Amigo, B.; Bianchini, P.; Diaspro, A.; Iagatti, A.; Patrizi, B.; Foggi, P.; Agut, M.; Nonell, S.; Abbruzzetti, S.; Viappiani, C. Subdiffraction localization of a nanostructured photosensitizer in bacterial cells *Scientific Reports* **2015**, *5*, 15564.

(18) Lepeshkevich, S. V.; Parkhats, M. V.; Stasheuski, A. S.; Britikov, V. V.; Jarnikova, E. S.; Usanov, S. A.; Dzhagarov, B. M. Photosensitized Singlet Oxygen Luminescence from the Protein Matrix of Zn-Substituted Myoglobin *Journal of Physical Chemistry A* **2014**, *118*, 1864-1878.

(19) Adamsen, C. E.; Møller, J. K. S.; Parolari, G.; Gabba, L.; Skibsted, L. H. Changes in Zn-porphyrin and proteinous pigments in italian dry-cured ham during processing and maturation *Meat Science* **2006**, *74*, 373-379.

(20) Parolari, G.; Benedini, R.; Toscani, T. Color Formation in Nitrite-Free Dried Hams as Related to Zn-Protoporphyrin IX and Zn-Chelatase Activity *Journal of Food Science* **2009**, *74*, C413-C418.

(21) Wakamatsu, J.-i.; Uemura, J.; Odagiri, H.; Okui, J.; Hayashi, N.; Hioki, S.; Nishimura, T.; Hattori, A. Formation of zinc protoporphyrin IX in Parma-like ham without nitrate or nitrite *Animal Science Journal* **2009**, *80*, 198-205.

(22) Wakamatsu, J.-i.; Odagiri, H.; Nishimura, T.; Hattori, A. Quantitative determination of Zn protoporphyrin IX, heme and protoporphyrin IX in Parma ham by HPLC *Meat Science* **2009**, *82*, 139-142.

(23) Grossi, A. B.; do Nascimento, E. S. P.; Cardoso, D. R.; Skibsted, L. H. Proteolysis involvement in zinc protoporphyrin IX formation during Parma ham maturation *Food Research International* **2014**, *56*, 252-259.

(24) Adamsen, C. E.; Møller, J. K. S.; Hismani, R.; Skibsted, L. H. Thermal and photochemical degradation of myoglobin pigments in relation to colour stability of sliced dry-cured Parma ham and sliced dry-cured ham produced with nitrite salt *European Food Research and Technology* **2004**, *218*, 403-409.

(25) Ascoli, F.; Rossi Fanelli, M. R.; Antonini, E. In *Methods in Enzymology*; Academic Press: 1981; Vol. Volume 76, p 72-87.

(26) Harrison, S. C.; Blout, R. Reversible conformational changes of myoglobin and apomyoglobin *Journal of Biological Chemistry* **1965**, *240*, 299-303.

(27) Abbruzzetti, S.; Bruno, S.; Faggiano, S.; Grandi, E.; Mozzarelli, A.; Viappiani, C. Time-resolved methods in Biophysics. 2. Monitoring haem proteins at work with nanosecond laser flash photolysis *Photochemical and Photobiological Sciences* **2006**, *5*, 1109-1120.

(28) Nonell, S.; Braslavsky, S. E. In *Singlet oxygen, UV-A, and Ozone*; Sies, L. P. a. H., Ed.; Academic Press: San Diego, 2000; Vol. 319, p 37–49.

(29) Zemel, H.; Hoffman, B. M. Long-range triplet-triplet energy transfer within metal-substituted hemoglobins *Journal of the American Chemical Society* **1981**, *103*, 1192-1201.

(30) Nonell, S.; Braslavsky, S. E. Time-resolved singlet oxygen detection *Methods in Enzymology* **2000**, *319*, 37-49.

(31) Maisch, T.; Baier, J. r.; Franz, B.; Maier, M.; Landthaler, M.; Szeimies, R.-M.; BÃ¤umler, W. The role of singlet oxygen and oxygen concentration in photodynamic inactivation of bacteria *Proceedings of the National Academy of Sciences* **2007**, *104*, 7223-7228.

(32) Sperandio, F. F.; Huang, Y.-Y.; Hamblin, M. R. Antimicrobial Photodynamic Therapy to Kill Gram-negative Bacteria *Recent patents on anti-infective drug discovery* **2013**, *8*, 108-120.

(33) Ogilby, P. R. Singlet oxygen: there is indeed something new under the sun *Chemical Society Reviews* **2010**, *39*, 3181-3209.

(34) Demidova, T. N.; Hamblin, M. R. Photodynamic Inactivation of Bacillus Spores, Mediated by Phenothiazinium Dyes *Applied and Environmental Microbiology* **2005**, *71*, 6918-6925.

(35) Ishikawa, S.-i.; Suzuki, K.; Fukuda, E.; Arihara, K.; Yamamoto, Y.; Mukai, T.; Itoh, M. Photodynamic antimicrobial activity of avian eggshell pigments *FEBS Letters* **2010**, *584*, 770-774.

Figure Captions

Figure 1. Absorption (blue) and fluorescence emission (black) spectra for ZnMb (4 μM) in PBS buffer. T=20°C.

Figure 2. Comparison of selected images acquired using a confocal microscope: transmitted light (A, D); confocal fluorescence (B, E) exploiting the emission of ZnMb under excitation at 561 nm and detection at 600-670 nm; transmitted light and fluorescence overlay (C, F) of the portions marked in A and D. Cell contours are marked with a dashed line. Pixel size 62x62nm; pixel dwell time 42 μs. A – B: *S. aureus* cells incubated with 1μM ZnMb; C – D: *S. aureus* cells incubated with 1 μM ZnMb and washed by means of centrifugation. The color bars are in arbitrary units. The scale bars are 5 μm.

Figure 3. Comparison of selected images acquired using a transmitted light (A, D) and a confocal fluorescence (B, E) microscope exploiting the emission of ZnMb under excitation at 561 nm and detection at 600-670 nm; transmitted light and fluorescence overlay (C, F) of the portions marked in A and D. Cell contours are marked with a dashed line. Pixel size 62x62nm; pixel dwell time 42 μs. A – B: *E. coli* cells incubated with 1 μM ZnMb; C – D: *E. coli* cells incubated with 1μM ZnMb and washed by means of centrifugation. The colors bar are in arbitrary unit. The scale bars are 5 μm.

Figure 4: Comparison of fluorescence emission spectra (panels A and C) and time-resolved singlet oxygen phosphorescence traces (panels B and D) for ZnMb in PBS buffer (black), ZnMb incubated with *S. aureus* (blue, panels A and B) or *E. coli* (blue, panels C and D) and ZnMb incubated with bacteria and washed (red). A fluorescence spectrum for the supernatant is reported in green in panel A. Fit curves for phosphorescence kinetics are reported for ZnMb in PBS (yellow) and ZnMb incubated with bacteria (orange). All samples are air-equilibrated at room temperature with [ZnMb] = 10 μM. Fluorescence spectra are collected under excitation at 552 nm. Phosphorescence kinetics are collected under excitation at 532 nm, detection at 1270 nm, with 256 ns resolution and 10 min acquisition at 1 kHz repetition rate.

Figure 5. Light fluence (at 520 nm) effect on *S. aureus* (A) and *E. coli* (C) incubated with ZnMb 3 μM (red), 10 μM (green), 20 μM (blue), 50 μM (magenta). Control experiments are performed without addition of ZnMb (black). ZnMb concentration effect on *S. aureus* (B) and *E. coli* (D) at 18 J/cm^2 (orange) and 37 J/cm^2 (violet) light fluences. Control experiments are performed in the dark (black).

Table 1. Photophysical parameters for ZnMb in PBS buffer and ZnMb incubated with *E. coli* and *S. aureus*.

Sample	τ_F (ns)	D ($\mu m^2/s$)	τ_T (µs) air equilibrated	τ_T (ms) nitrogen saturated	τ_Δ (µs)
ZnMb	2.0±0.1[$]		26±1*	13±1*	2.6±0.3[£]
			19±2[£]		
ZnMb with *E. coli*	2.1±0.1[$]	0.12±0.02[$]	29±3*	11±1*	2.6±0.3[£]
			20±2[£]		
ZnMb with *S. aureus*	2.1±0.1[$]	0.31±0.05[$]	34±3*	13±1*	2.6±0.3[£]
			22±2[£]		

[$]: FCS / TCSPC λ_{exc}=475 nm, λ_{det}=650-700 nm, 20 MHz, [ZnMb]≈1 µM ;*: LFP λ_{exc}=532 nm, λ_{det}=465 nm, [ZnMb]=2 or 5 µM ; [£]: TRP λ_{exc}=532 nm, λ_{det}=1275 nm, 1 KHz rep. rate, 10 min acquisition time, [ZnMb]=10 µM; deoxygenation: 1 hour flux pure nitrogen.

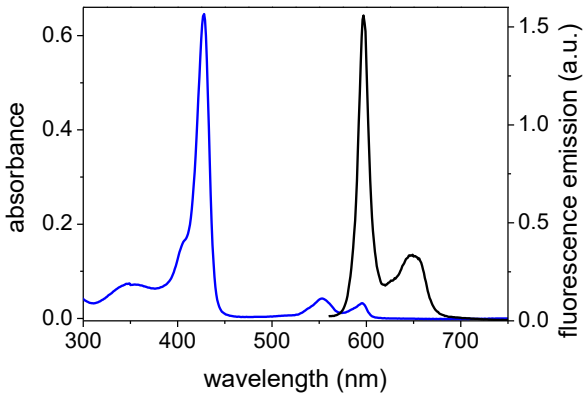

448

449 **Figure 1.**

450

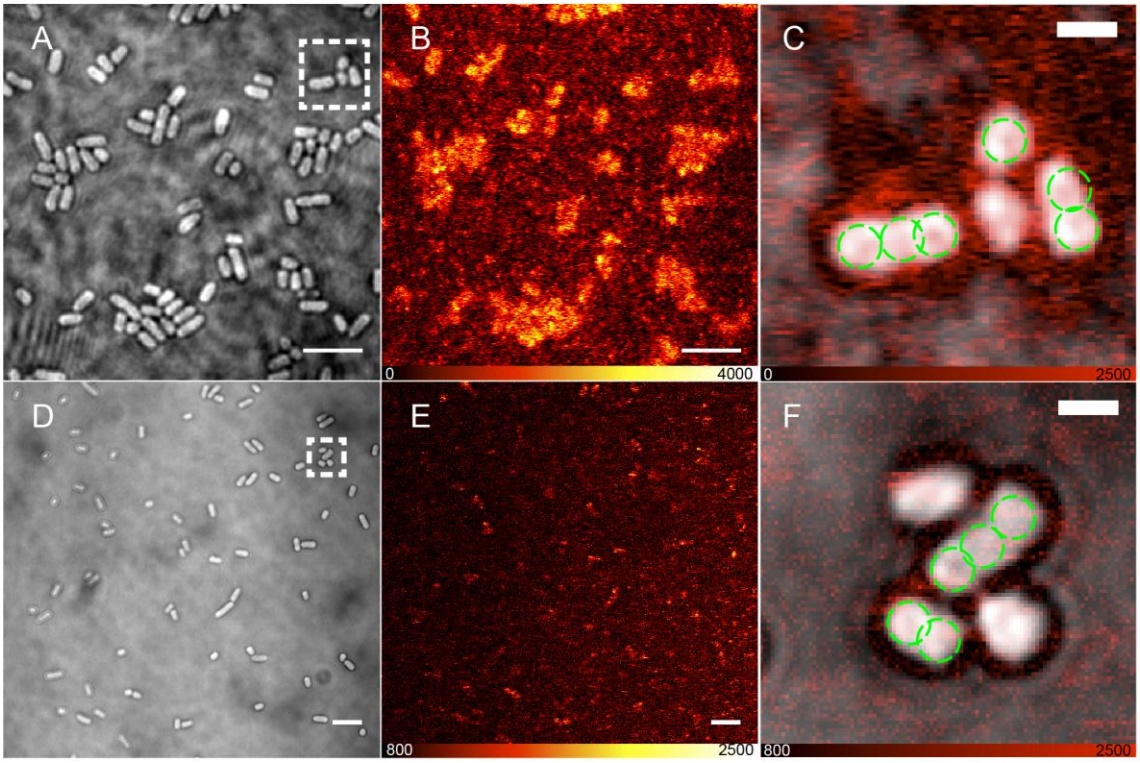

Figure 2.

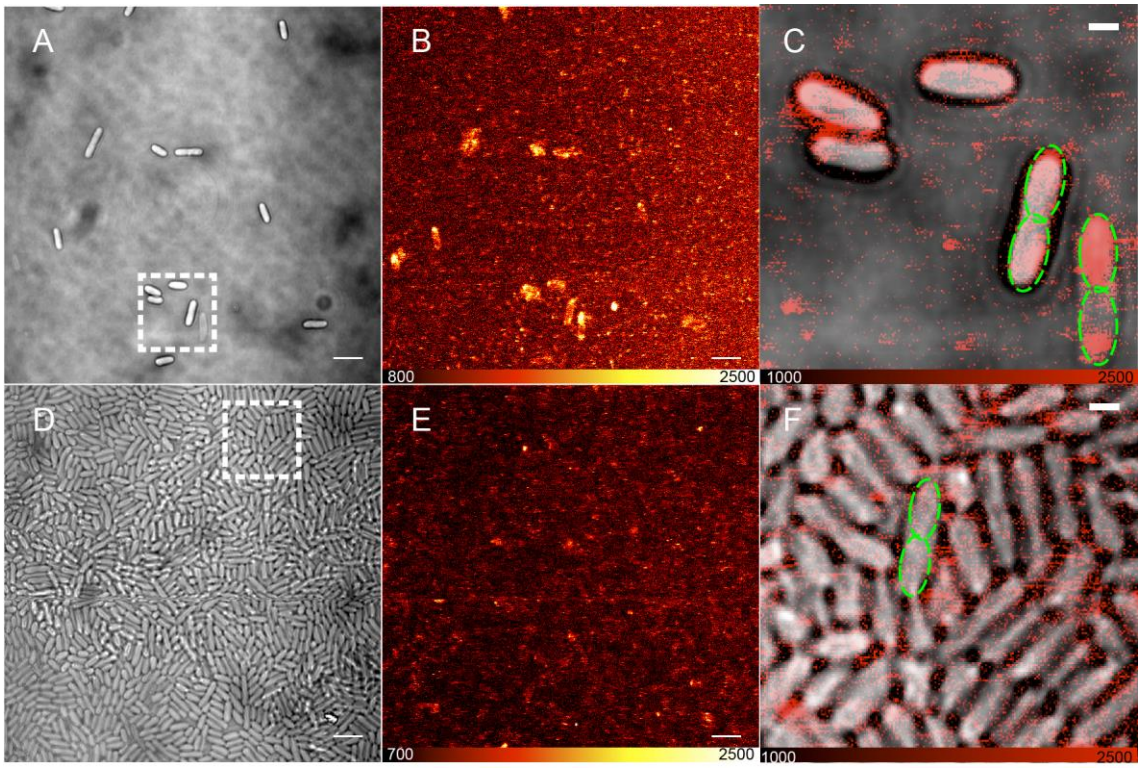

454

455 **Figure 3.**

456

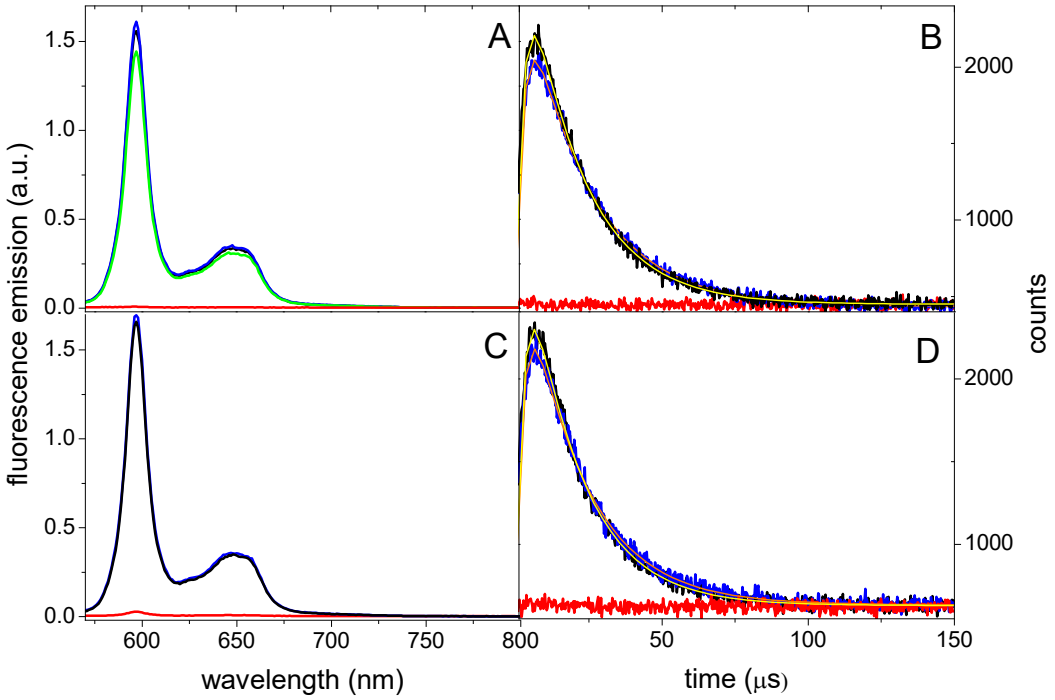

457
458

459 **Figure 4**.

460

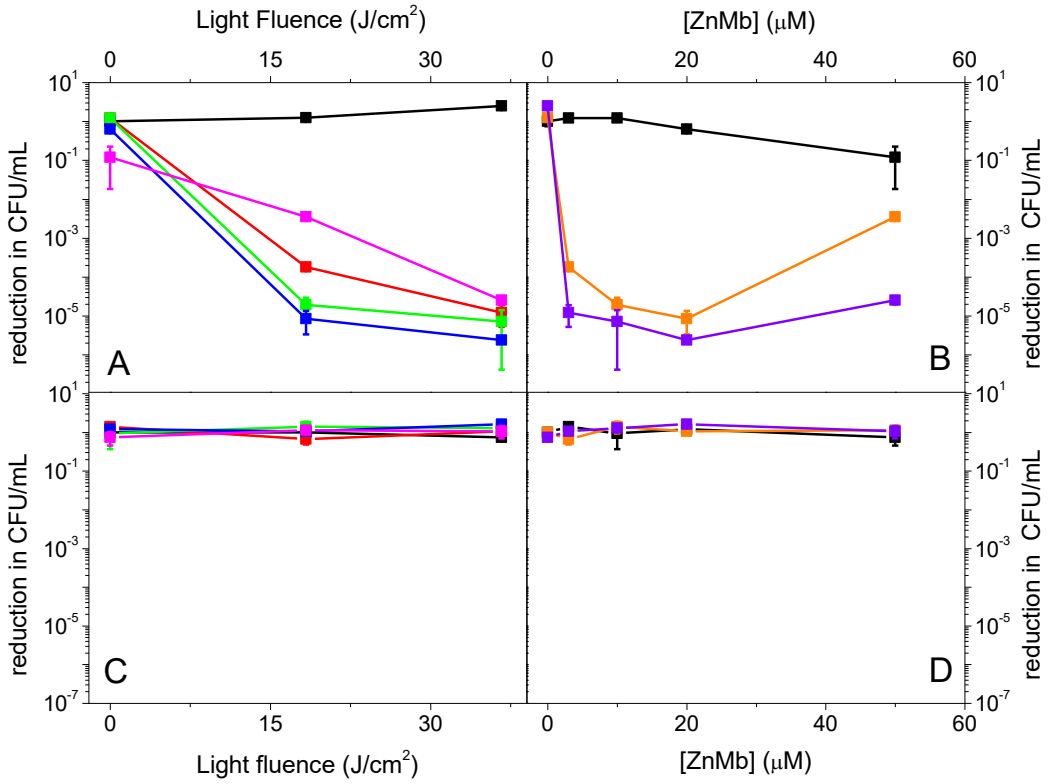

461
462

463 **Figure 5**.

464

465 Table of Contents Graphics

466